Supplementary Material

Table S1. Calculation of the $\Delta\chi$ tensors for yCc. $\Delta\chi_{ax}$ and $\Delta\chi_{rh}$ are the axial and rhombic components of the $\Delta\chi$ tensor in units of 10^{-32} m^3; α, β, and γ are the Euler angles (in degrees) relating the $\Delta\chi$-tensor frame to the molecular coordinate system; the angle $\kappa = (\alpha + \gamma) - \pi$ approximates the rotation of the orthogonal x' and y' $\Delta\chi$ axes relative to the molecular frame x and y axes (Fig. 3B). Errors are estimated as explained in the Experimental Section.

Structure[a]	n[b]	Atoms	$\Delta\chi_{ax}$	error	$\Delta\chi_{rh}$	error	α	error	β	error	γ	error	κ	error	σ^{2c}
X-ray, red (1YCC)	88	HN	3.20	0.09	1.31	0.14	120.4	5.6	11.1	0.7	67.9	7.6	8.3	4.7	
	171	N,HN	3.51	0.09	1.53	0.12	146.7	2.4	16.9	0.9	27.2	3.6	-6.1	2.2	
	88	CO	3.03	0.09	1.72	0.13	133.9	3.1	17.3	0.9	59.1	3.8	13.0	2.5	
	100	C_α	3.11	0.11	1.89	0.14	123.8	5.5	12.5	0.9	66.5	5.7	10.3	3.9	
	188	CO,C_α	3.06	0.07	1.92	0.11	132.2	3.5	14.9	0.8	58.8	3.8	11.0	2.6	
	278	CO,C_α,C_β	3.09	0.06	1.80	0.11	134.1	2.7	14.5	0.6	58.2	3.0	12.3	2.0	
	174	HN,CO	3.17	0.06	1.67	0.11	129.7	2.8	16.2	0.7	62.8	3.7	12.6	2.3	
	187	HN,C_α	3.16	0.07	1.73	0.14	122.8	4.6	12.0	0.6	66.6	4.9	9.4	3.4	
	272	HN,CO,C_α	3.11	0.06	1.87	0.11	130.5	2.9	14.3	0.6	60.9	3.7	11.4	2.3	
	362	HN,CO,C_α,C_β	3.12	0.05	1.80	0.10	133.0	2.9	14.3	0.5	59.2	3.1	12.1	2.1	
X-ray, red (1YCC)	446	N,HN,CO,C_α,C_β	3.17	0.05	1.80	0.09	135.5	2.3	15.1	0.5	55.8	2.5	11.3	1.7	0.046
X-ray, ox (2YCC)	449	N,HN,CO,C_α,C_β	3.12	0.05	1.46	0.08	139.6	1.8	18.1	0.5	55.7	2.4	15.2	1.5	0.050
NMR, red (1YFC)[d]	448	N,HN,CO,C_α,C_β	2.99	0.05	1.46	0.08	102.4	2.3	13.6	0.4	79.6	2.7	2.0	1.8	0.055
NMR, ox (1YIC)[d]	443	N,HN,CO,C_α,C_β	2.96	0.05	1.43	0.08	103.5	3.8	9.5	0.4	64.7	4.1	11.8	2.8	0.051
Average[e]		N,HN,CO,C_α,C_β	**3.06**	**0.10**	**1.54**	**0.17**	**120.2**	**20.1**	**14.1**	**3.6**	**63.9**	**11.3**	**10.1**	**2.8**	**0.050**

[a] yCc structure used in the $\Delta\chi$ tensor calculations. [b] Number of atoms used in the fitting. [c] Statistical variance given by $\sigma^2 = \frac{1}{n-5}\sum(\Delta\delta_{obs} - \delta_{PCS}^{calc})^2$, with the summation carried over all atoms used in the fitting. [d] Average NMR structure used in the calculations. [e] The average values of the $\Delta\chi$ parameters obtained from four yCc structures; the errors are the standard deviations.

Table S2. Calculation of the $\Delta\chi$ tensors for hCc. $\Delta\chi_{ax}$ and $\Delta\chi_{rh}$ are the axial and rhombic components of the $\Delta\chi$ tensor in units of 10^{-32} m^3; α, β, and γ are the Euler angles (in degrees) relating the $\Delta\chi$-tensor frame to the molecular coordinate system; the angle $\kappa = (\alpha + \gamma) - \pi$ approximates the rotation of the orthogonal x' and y' $\Delta\chi$ axes relative to the molecular frame x and y axes (Fig. 3B). A set of N, HN, CO, C_α, and C_β atoms was used in the calculations. Errors are estimated as explained in the Experimental Section.

Structure[a]	n[b]	$\Delta\chi_{ax}$	error	$\Delta\chi_{rh}$	error	α	error	β	error	γ	error	κ	error	σ^{2c}
X-ray, ox (1HRC)	425	3.10	0.05	1.50	0.13	126.9	3.1	11.4	0.5	62.0	2.9	8.9	2.1	0.060
NMR, ox (1AKK)[d]	439	3.29	0.06	1.10	0.07	131.2	2.5	11.9	0.5	53.3	2.7	4.6	1.9	0.075
NMR, red (1GIW)[d]	440	2.93	0.05	1.00	0.06	111.8	3.6	11.4	0.5	68.1	4.2	-0.1	2.7	0.082
NMR, ox (1OCD)[d]	425	2.10	0.06	1.26	0.08	160.3	2.1	21.8	1.0	37.9	2.5	18.2	1.6	0.095
NMR, red (2FRC)[d]	421	2.92	0.07	0.71	0.06	130.0	2.4	17.3	0.6	50.6	4.5	0.6	2.5	0.085
Average[e]		**2.87**	**0.46**	**1.11**	**0.29**	**132.0**	**17.6**	**14.7**	**4.7**	**54.4**	**11.5**	**6.4**	**7.5**	**0.079**

[a] hCc structure used in the $\Delta\chi$ tensor calculations. [b] Number of atoms used in the fitting. [c] Statistical variance given by $\sigma^2 = \frac{1}{n-5}\sum(\Delta\delta_{obs} - \delta_{PCS}^{calc})^2$, with the summation carried over all atoms used in the fitting. [d] Average NMR structure used in the calculations. [e] The average values of the $\Delta\chi$ parameters obtained from five hCc structures; the errors are the standard deviations.

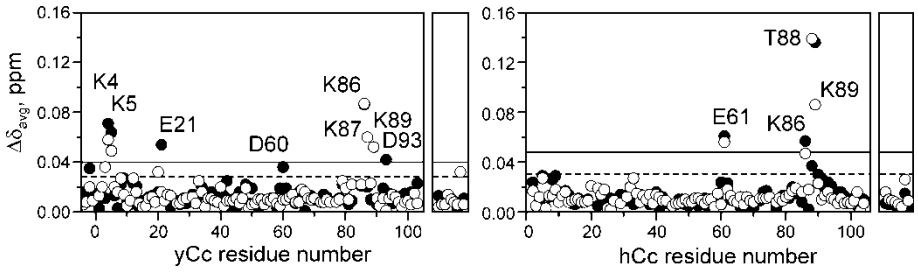

Fig. S1. Salt-induced chemical shift perturbations ($\Delta\delta_{avg}$) of NH atoms of (A) yCc and (B) hCc in the oxidized (open symbols) and reduced (filled symbols) states. In each panel, the main plot and right-side insert show $\Delta\delta_{avg}$ for backbone amides and side-chain NH_2 groups of Asn and Gln residues, respectively. $\Delta\delta_{avg}$ is defined as $\Delta\delta_{\mathrm{avg}} = \sqrt{((\Delta\delta_N/5)^2 + \Delta\delta_{\mathrm{HN}}^2)/2}$, where $\Delta\delta_{\mathrm{N}}$ and $\Delta\delta_{\mathrm{HN}}$ are the salt-induced chemical shifts of N and HN nuclei, respectively. Horizontal lines denote an average plus one (dashed) or two (solid) standard deviations calculated over all values in a dataset. Outliers are indicated by the labels.

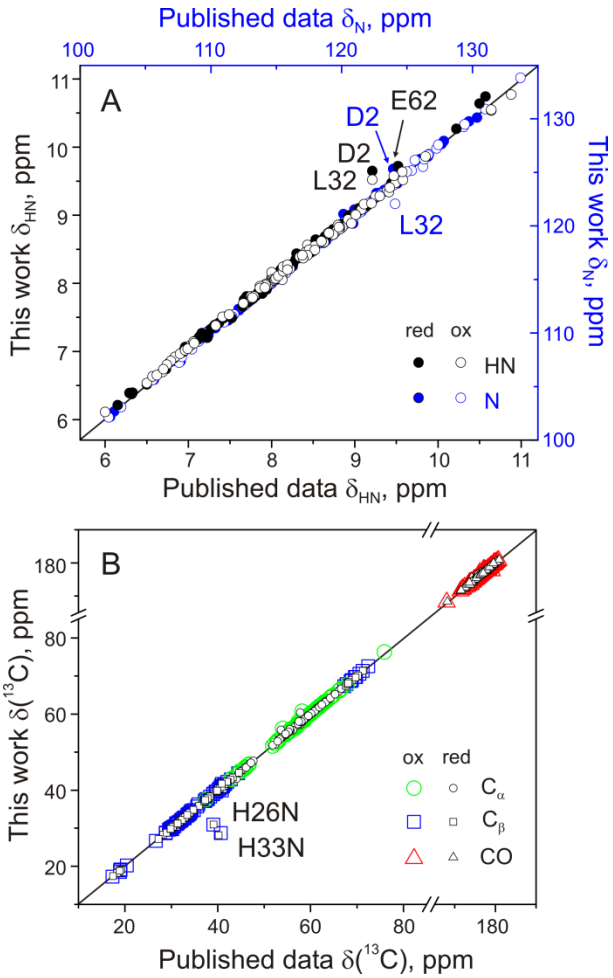

Fig. S2. Comparison of the chemical shift assignments of hCc obtained in this and an earlier work (Liu et al. 2003). (A) Chemical shifts of HN (black) and N (blue) atoms of the reduced (filled circles) and oxidized (open circles) hCc as compared to the published data (BMRB entries 5829 and 5830, respectively; Liu et al. 2003). (B) Chemical shifts of CO (triangles), C_α (circles), and C_β (squares) atoms of reduced (black-and-white symbols) and oxidized (coloured symbols) hCc as compared to the published data for H26N/H33N hCc variant (BMRB entries 5827 and 5828, respectively; Liu et al. 2003). The most prominent outliers are indicated by the labels.

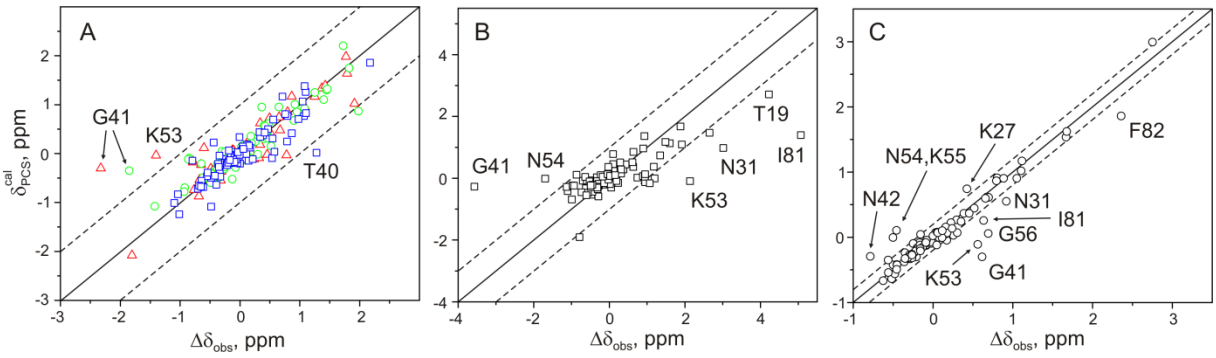

Fig. S3. Comparison of the obsreved differences in chemical shifts between the oxidized and reduced hCc ($\Delta\delta_{obs}$) and calculated PCSs (δ_{PCS}^{cal}). The latter values were obtained for (A) CO (red triangles), C_α (green circles), C_β (blue squares); (B) N; and (C) HN atoms from the X-ray structure of hCc^{ox} and the corresponding $\Delta\chi$ tensor determined in this study. Dashed lines indicate cut-offs used in the $\Delta\chi$ tensor fitting (see Experimental Section). The most prominent outliers are indicated by the labels.

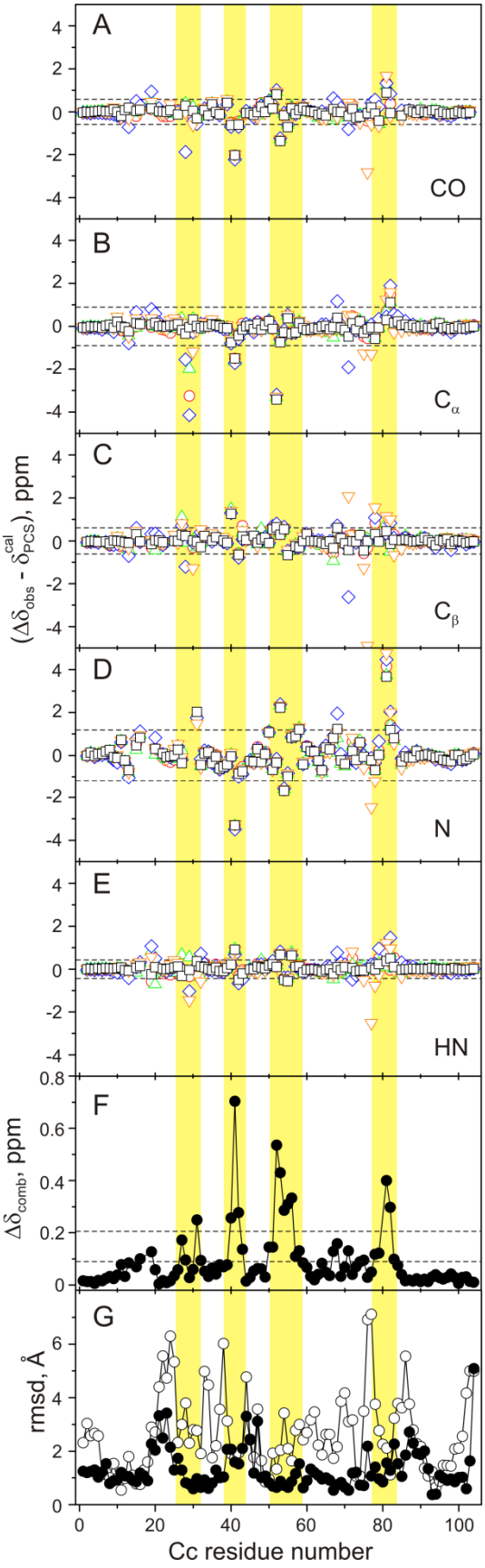

Fig. S4. Distribution of hCc residues involved in redox-dependent changes as determined by paramagnetic NMR spectroscopy (this work, A-F) and conventional structural analyses (previous studies, G). (A-E) Distribution of $\left(\Delta\delta_{obs} - \delta_{PCS}^{cal}\right)$ terms for (A) CO, (B) C_α, (C) C_β, (D) N, and (E) HN atoms as a function of hCc residue number. Dashed lines denote the average plus one standard deviation calculated over all atoms in a given category. δ_{PCS}^{cal} values were computed from the X-ray structure (black squares, hCc^{ox}) or NMR structures of Banci *et al.* (red circles – hCc^{ox}; green triangles – hCc^{red}) and Wand and co-workers (blue diamonds – hCc^{ox}; orange inverted triangles – hCc^{red}) using the $\Delta\chi$ tensors determined in this work. (F) The combined, per-residue difference between $\Delta\delta_{obs}$ and δ_{PCS}^{cal}, $\Delta\delta_{comb}$, as defined in Equation 7. Dashed lines denote the average and the average plus one standard deviation. Stretches of residues exhibiting redox-dependent changes are highlighted. (G) Pairwise backbone root-mean-square deviations between the NMR structures of the reduced and oxidized hCc determined by Banci *et al.* (filled symbols) and Wand and co-workers (open symbols).

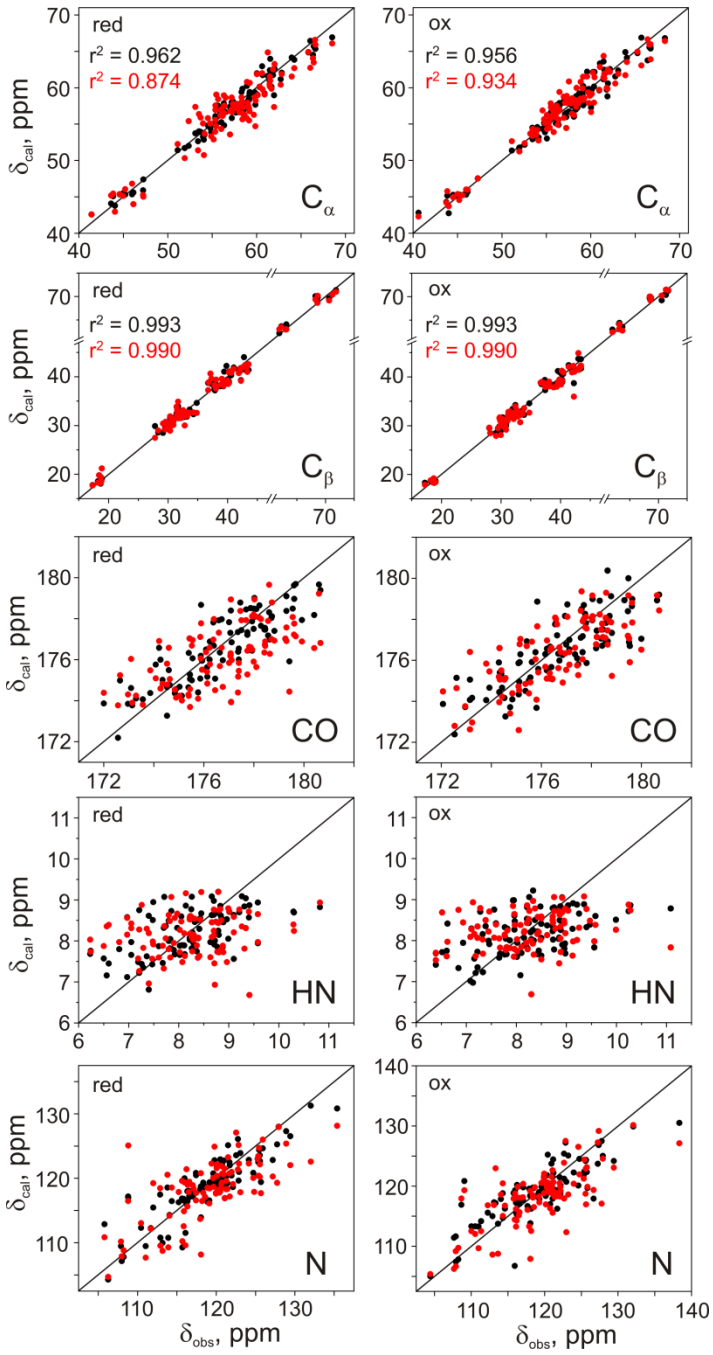

Fig. S5. Comparison of the experimental diamagnetic chemical shifts (δ_{obs}) for yCc^{red} (left panels) and yCc^{ox} (right panels) with those calculated from the X-ray (black) or NMR (red) structures (δ_{calc}). In the plots for C_α and C_β atoms, the correlation coefficients for the y = x line are indicated. Residues C14, C17, H18, and M80 (ligands to the haem) were excluded from the analysis.